



Rezansoff, A. M., Laing, R. and Gilleard, J. S. (2016) Evidence from two independent backcross experiments supports genetic linkage of microsatellite Hcms8a20, but not other candidate loci, to a major ivermectin resistance locus in *Haemonchus contortus*. *International Journal for Parasitology*, 46(10), pp. 653-661. (doi:[10.1016/j.ijpara.2016.04.007](https://doi.org/10.1016/j.ijpara.2016.04.007))

There may be differences between this version and the published version. You are advised to consult the publisher's version if you wish to cite from it.

<http://eprints.gla.ac.uk/129699/>

Deposited on: 22 October 2019

Enlighten – Research publications by members of the University of Glasgow  
<http://eprints.gla.ac.uk>

1 **Evidence from two independent backcross experiments supports genetic linkage of microsatellite**  
2 **Hcms8a20, but not other candidate loci, to a major ivermectin resistance locus in *Haemonchus***  
3 ***contortus***

4

5 Andrew M. Rezansoff<sup>a</sup>, Roz Laing<sup>b</sup>, John S. Gilleard<sup>a,\*</sup>

6 <sup>a</sup>*Department of Comparative Biology and Experimental Medicine, Faculty of Veterinary Medicine,*  
7 *University of Calgary, Alberta, Canada*

8 <sup>b</sup>*Institute of Biodiversity, Animal Health and Comparative Medicine, College of Medical, Veterinary*  
9 *and Life Sciences, University of Glasgow, Scotland, UK*

10 \* Corresponding author. Professor John Gilleard, Department of Comparative Biology and  
11 Experimental Medicine, Faculty of Veterinary Medicine, 3330, Hospital Drive, University of Calgary,  
12 Calgary, Alberta, T2N 4N1 Canada  
13 Tel.: +1 (403) 210 6327; fax: +1 (403) 210 7882.

14 *E-mail address:* [jsgillea@ucalgary.ca](mailto:jsgillea@ucalgary.ca)

15

16

17 **Abstract**

18 *Haemonchus contortus* is the leading parasitic nematode species used to study anthelmintic  
19 drug resistance. A variety of candidate loci have been implicated as being associated with ivermectin  
20 resistance in this parasite but definitive evidence of their importance is still lacking. We have  
21 previously performed two independent serial backcross experiments to introgress ivermectin resistance  
22 loci from two *H. contortus* ivermectin-resistant strains - MHco4(WRS) and MHco10(CAVR) - into the  
23 genetic background of the ivermectin-susceptible genome reference strain MHco3(ISE). We have  
24 interrogated a number of candidate ivermectin resistance loci in the resulting backcross populations and  
25 assessed the evidence for their genetic linkage to an ivermectin resistance locus. These include the  
26 microsatellite marker Hcms8a20 and six candidate genes *Hco-glc-5*, *Hco-avr-14*, *Hco-lgc-37*  
27 (previously designated *Hco-hg-1*), *Hco-pgp-9* (previously designated *Hco-pgp-1*), *Hco-pgp-2* and *Hco-*  
28 *dyf-7*. We have sampled the haplotype diversity of amplicon markers within, or adjacent to, each of  
29 these loci in the parental strains and fourth generation backcross populations to assess the evidence for  
30 haplotype introgression from the resistant parental strain into the genomic background of the  
31 susceptible parental strain in each backcross. The microsatellite Hcms8a20 locus showed strong  
32 evidence of such introgression in both independent backcrosses, suggesting it is linked to an important  
33 ivermectin resistance mutation in both the MHco4(WRS) and MHco10(CAVR) strains. In contrast,  
34 *Hco-glc-5*, *Hco-avr-14*, *Hco-pgp-9* and *Hco-dyf-7* showed no evidence of introgression in either  
35 backcross. *Hco-lgc-37* and *Hco-pgp-2* showed only weak evidence of introgression in the MHco3/4  
36 backcross but not in the MHco3/10 backcross. Overall, these results suggest that microsatellite marker  
37 Hcms8a20, but not the other candidate genes tested, is linked to a major ivermectin resistance locus in  
38 the MHco4(WRS) and MHco10(CAVR) strains. This work also emphasizes the need for genome-wide  
39 approaches to identify mutations responsible for the ivermectin resistance in this parasite.

40 *Keywords: Haemonchus contortus; Nematode; Ivermectin; Anthelmintic; Drug resistance*

## 41 1. Introduction

42 Identifying genetic markers of anthelmintic resistance is a key research priority in order to  
43 provide tools to monitor and manage its emergence and spread (James et al., 2009; Beech et al., 2011).  
44 Anthelmintic resistance is widespread in *Haemonchus contortus*, a parasitic nematode of small  
45 ruminants that has been a leading model for the study of resistance to ivermectin, one of the most  
46 important drugs used in human and animal helminth control (Kaplan and Vidyashankar, 2012; Gilleard,  
47 2013). There have been many efforts over the last two decades to test specific candidate genes for  
48 associations with ivermectin resistance in *H. contortus* (Gilleard, 2013). These candidate genes have  
49 been chosen largely on the basis of having potential roles as drug targets or in drug efflux (Gilleard,  
50 2006; Gilleard and Beech, 2007). Although evidence of selection by ivermectin treatment has been  
51 suggested for a number of such loci, their roles in resistance have not yet been conclusively  
52 demonstrated (Gilleard, 2006; Gilleard and Beech, 2007).

53 In the study presented here, we examine seven genetic loci previously suggested to be  
54 associated with ivermectin resistance in *H. contortus*; a microsatellite marker Hcms8a20 and six  
55 candidate genes, *Hco-avr-14*, *Hco-glc-5*, *Hco-lgc-37*, *Hco-pgp-9*, *Hco-pgp-2* and *Hco-dyf-7*. For each  
56 of these loci, we have investigated evidence for genetic linkage to a major ivermectin resistance locus  
57 in two ivermectin-resistant strains, MHco4(WRS) and MHco10(CAVR). These strains are commonly  
58 used in resistance studies and were originally derived as field populations from different continents  
59 (Redman et al., 2008). We have used two previously characterised ivermectin-resistant *H. contortus*  
60 populations - MHco3/4.BC and MHco3/10.BC - that were independently derived by serial  
61 backcrossing of the MHco4(WRS) and MHco10(CAVR) resistant strains against the MHco3(ISE)  
62 susceptible strain, respectively (Redman et al., 2012). For each of the candidate loci, we evaluated the  
63 evidence for introgression of haplotypes from the resistant parental strains into the fourth generation

64 backcross populations in order to determine whether they are located in a region of the genome linked  
65 to a major ivermectin resistance locus (Redman et al., 2012).

66 The basis on which each of the candidate loci have been previously implicated in ivermectin  
67 resistance is briefly explained here. The Hcms8a20 microsatellite was the only one out of 18  
68 microsatellite loci that showed evidence of genetic introgression in the two independent backcross  
69 experiments undertaken to map ivermectin resistance loci in the MHco4(WRS) and MHco10(CAVR)  
70 strains [strains?] (Redman et al 2012). *Hco-avr-14* and *Hco-glc-5* are members of the *H. contortus*  
71 glutamate-gated chloride channel (GLC) family (Wolstenholme and Rogers, 2005; McCavera et al.,  
72 2007; Laing et al., 2013). Three members of this family in *Caenorhabditis elegans* - *Cel-glc-1*, *Cel-*  
73 *avr-14* and *Cel-avr-15* - have been shown to be ivermectin targets by genetic mutation and  
74 complementation studies (Dent et al., 2000; Ghosh et al., 2012). The *H. contortus* homologue of *Cel-*  
75 *avr-14* - *Hco-avr-14* - was implicated in ivermectin resistance by its ability to rescue ivermectin  
76 susceptibility when heterologously expressed in *C. elegans*, suggesting it is an ivermectin target in the  
77 parasite (McCavera et al., 2007, 2009; Glendinning et al., 2011). *Hco-glc-5* was implicated by the  
78 observation of haplotype frequency changes during experimental passage of an *H. contortus* strain  
79 under ivermectin selection (Blackhall et al., 1998a). *Hco-lgc-37* - a gamma aminobutyric acid  
80 (GABA)-gated chloride channel renamed from *Hco-hg-1* (Beech et al., 2010a) - was also implicated  
81 using the same approach and strains (Blackhall et al., 2003). A subsequent study has also presented  
82 evidence that certain alleles of both *Hco-glc-5* and *Hco-lgc-37* were associated with reduced sensitivity  
83 of adult feeding and larval movement to moxidectin (Beech et al., 2010b).

84 *Hco-pgp-9* and *Hco-pgp-2* are members of the P-glycoprotein (PGP) trans-membrane  
85 transporter family. *Hco-pgp-9* and *Hco-pgp-2* were originally designated as *Hco-pgp-1* and *Hco-pgp-A*,  
86 respectively (Xu et al., 1998; Le Jambre et al., 1999), but were subsequently re-named based on the  
87 identification of their respective *C. elegans* orthologues (Williamson and Wolstenholme, 2012). This

88 gene family, known to be involved in ivermectin efflux in mammals (Schinkel, 1999), has been  
89 suggested to be involved in ivermectin resistance in parasitic nematodes in a number of studies and  
90 reviews (Blackhall et al., 1998b; Xu et al., 1998; Le Jambre et al., 1999, Sangster et al., 1999; Bartley  
91 et al., 2009; Williamson and Wolstenholme, 2012). In the case of *Hco-pgp-2*, Blackhall et al. (1998b)  
92 used the same methodology and strains as used for *Hco-glc-5* and *Hco-lgc-37*. As with the two  
93 previously examined candidate genes, they showed that a single *Hco-pgp-2* haplotype had a  
94 significantly higher frequency in the ivermectin selected population compared with the non-selected  
95 population (Blackhall et al., 1998b). *Hco-pgp-9* was independently implicated in ivermectin resistance  
96 by the observation that populations of *H. contortus*/*Haemonchus placei* hybrid F1 progeny that  
97 survived ivermectin treatment contained a higher frequency of *Hco-pgp-9* alleles derived from the  
98 resistant *H. contortus* parental strain than from the susceptible *H. placei* parental strain (Le Jambre et  
99 al., 1999).

100 The most recent candidate gene to be implicated in ivermectin resistance is *Hco-dyf-7*, a gene  
101 which encodes a protein required for proper dendritic anchoring and migration of amphid neurons  
102 (Heiman and Shaham, 2009). This gene has recently been proposed to have an important, and possibly  
103 global, role in ivermectin resistance (Urdaneta-Marquez et al., 2014). Classical genetic mapping and  
104 transgenic rescue experiments showed that loss-of-function of the *Cel-dyf-7* gene confers ivermectin  
105 resistance in *C. elegans* (Urdaneta-Marquez et al., 2014). In the same study, an orthologue of this *C.*  
106 *elegans* gene was identified in *H. contortus*, *Hco-dyf-7*. A specific haplotype of this *H. contortus* gene,  
107 defined by 15 single nucleotide polymorphisms (SNP)s, was shown to increase in frequency during  
108 ivermectin selection using the same parasite strains as had been previously used by Blackhall et al.  
109 (1998a, 1998b, 2003) for *Hco-glc-5*, *Hco-lgc-37* and *Hco-pgp-2*. In addition, several - although not all -  
110 of the SNPs that defined this haplotype were reported to occur more frequently in a panel of

111 ivermectin-resistant *H. contortus* field populations compared with several susceptible populations  
112 (Urdaneta-Marquez et al., 2014).

113 In summary, there is circumstantial, but not conclusive, evidence for the potential association of  
114 a number of different *H. contortus* candidate loci with ivermectin resistance. In this paper, we  
115 interrogate two previously validated independent backcross experiments for evidence of genetic  
116 linkage of each of these candidate loci to a major ivermectin resistance mutation. Our results support  
117 previous evidence that the microsatellite marker Hcms8a20 is linked to a major ivermectin resistance  
118 locus in the two ivermectin-resistant parental strains used in each backcross. In contrast, our results do  
119 not provide similar support for any of the other candidate loci tested.

120

## 121 **2. Materials and methods**

### 122 *2.1. Parasite populations and preparation of genomic DNA*

123 The backcross populations used in this study were derived from two independent backcross  
124 experiments between the susceptible genome reference strain - MHco3(ISE) (Laing et al., 2013) - and  
125 each of two independent ivermectin-resistant strains, MHco4(WRS) and MHco10(CAVR) (Redman et  
126 al., 2012). The MHco3(ISE) strain is susceptible to all the major anthelmintic classes and was  
127 originally derived from the ISE strain by multiple rounds of inbreeding before the genome project was  
128 commenced (Roos et al., 2004; Laing et al., 2013). MHco4(WRS) is derived from the White River  
129 Strain (WRS) originally isolated as an ivermectin-resistant field strain from South Africa (Van Wyk  
130 and Malan, 1988). MHco10(CAVR) is derived from the Chiswick Avermectin Resistant Strain  
131 (CAVR) strain originally isolated as an avermectin-resistant strain from the field in Australia (Le  
132 Jambre et al., 1995). Details of the genetic backcrossing strategy have been previously reported in  
133 Redman et al. (2012), so only a brief overview is given here. F1 progeny of parental crosses were

134 exposed to ivermectin by oral dosing and the survivors were then backcrossed against the susceptible  
135 MHco3(ISE) parental strain. Subsequent backcrossing of drug survivors was repeated for three more  
136 generations such that phenotypically resistant fourth generation backcross populations were obtained  
137 (MHco3/4.BC and MHco3/10.BC). These populations have an overall genetic background of the  
138 susceptible parental MHco3(ISE) strain as previously validated with microsatellite markers. However,  
139 they are phenotypically resistant to ivermectin, showing that ivermectin resistance loci have been  
140 introgressed from the original resistant parental strains (Redman et al., 2012). There was no evidence of  
141 sex linkage of the resistance trait from the backcrossing experiments. Pools of genomic DNA were  
142 created by combining lysates from the heads of 20 males and 20 females from each of the three  
143 parental populations - MHco3(ISE), MHco4(WRS) and MHco10(CAVR). The DNA lysis protocol has  
144 been previously described (Redman et al., 2008). The fourth generation backcrosses were  
145 experimentally passaged for one generation to increase worm numbers (Redman et al., 2012). Progeny  
146 of this passage (F2s of the fourth generation backcrosses) were selected with 0.1 mg/kg of ivermectin  
147 in vivo in a controlled efficacy test (Redman et al., 2012) from which drug surviving females were used  
148 to create lysate pools of the MHco3/4.BC and MHco3/10.BC backcrosses assessed in this study. Pools  
149 were created by combining genomic DNA (gDNA) of 33 and 26 drug surviving females of the  
150 MHco3/4.BC and MHco3/10.BC strains, respectively.

151

## 152 2.2. PCR amplification

153 Test PCR amplifications were carried out on the six candidate genes using primer pairs reported  
154 in previously published studies (Blackhall et al. 1998a, b, 2003; Jagannathan et al., 1999; Le Jambre et  
155 al., 1999; Urdaneta-Marquez et al., 2014). Only the *Hco-lgc-37* primer pair from Blackhall et al. (2003)  
156 amplified sufficiently robustly in all five populations and were used in this study. Geneious Pro version

157 6.1.6 was used to design new primer pairs for the other loci (<http://www.geneious.com>, Kearse et al.,  
158 2012) (Supplementary Table S1). These spanned at least one intron to ensure sufficient polymorphism  
159 was obtained in the amplified sequence. Primers were also designed to amplify a non-coding 725 bp  
160 fragment 1032 bases away from Hcms8a20, a microsatellite for which there was previous evidence of  
161 genetic linkage to an ivermectin resistance locus (Redman et al., 2012). PCRs were performed in 50  $\mu$ L  
162 reactions using 0.5  $\mu$ L of pooled gDNA template and Phusion High-Fidelity HF DNA Polymerase  
163 (New England Biolabs, USA country). The following thermocycling conditions were used: 98°C for 2  
164 min, (98°C for 10 s, 60°C for 30 s and 72°C for 30 s) for 35 cycles, 72°C for 5 min.

165

### 166 2.3. Cloning and sequencing of PCR amplicons

167 PCR products were gel purified using an e.Z.N.A MicroElute® Gel Extraction Kit (Omega  
168 Biotek, USAcountry) and then cloned into the pJET1.2/blunt cloning vector using a CloneJET PCR  
169 Cloning Kit (ThermoFisher Scientific, USAcountry). For each cloning plate, corresponding to each  
170 population/locus combination, 24 colonies were randomly selected and plasmid DNA purified using  
171 the e.Z.N.A Plasmid Mini-Kit I (Omega Biotek) (20 colonies were selected in the case of *Hco-dyf-7*).  
172 Plasmid clones were then sequenced using the T7(5'-TAATACGACTCACTATAGGG-3') forward  
173 primer on a BigDye Terminator Cycle Sequencing platform (Applied Biosystems, USAcountry). *Hco-*  
174 *pgp-9* clones required an additional (reverse) primer to sequence given its longer amplicon length  
175 (pJET1.2 reverse primer: 5'-AAGAACATCGATTTTCCATGGCAG-3').

176

### 177 2.4. DNA sequence analysis

178 All sequences were aligned using the MUSCLE alignment tool (Edgar, 2004) at default settings  
179 in Geneious Pro v. 6.1.6. Primer sequences were trimmed and the sequences were re-aligned.  
180 Polymorphisms appearing more than once in the sequence data set are expected to be real, whereas  
181 polymorphisms that only occur once are possible artefacts due to polymerase-induced errors (Chaudhry  
182 et al., 2015; Redman et al., 2015). Consequently, we only considered SNPs occurring more than once  
183 in the entire dataset in order to take a conservative approach and ensure only real polymorphisms were  
184 considered. Sequence alignments of both the unedited and edited sequences are presented in  
185 Supplementary Figs. S1, S2.

186 The frequency of each haplotype was determined at each locus for each population and this is  
187 referred to as the “haplotype profile”. Haplotypes were labelled alphabetically for each locus based on  
188 their rank frequency observed in the MHco3(ISE) population (Figs. 1 – 3). Remaining haplotypes not  
189 observed in MHco3(ISE) were labelled arbitrarily. The number of clones successfully sequenced and  
190 the number of different haplotypes observed at each locus were recorded for each strain (Table 1). For  
191 each locus, the number of haplotypes shared by the parental strains of a cross, together with the number  
192 of haplotypes unique to each parental strain of a cross, was also recorded (Table 1). Pairwise  $F_{st}$  values  
193 (calculated in Arlequin v. 3.1 at default settings; Excoffier et al., 2005) were used to quantify the level  
194 of similarity between haplotype profiles between parental and backcross populations for each amplicon  
195 marker. P-values of less than 0.05 were considered significant.

196

### 197 2.5. Chromosomal assignments for each amplicon marker

198 Chromosomal synteny is high between *H. contortus* and *C. elegans* (although gene order on a  
199 chromosome is generally poorly conserved) (Laing et al., 2011). Consequently, we inferred the  
200 chromosomal assignment for each amplicon marker based on the syntenic relationships with the *C.*

201 *elegans* orthologues of gene models present on the same *H. contortus* genomic scaffold. The closest 14  
202 gene models on the same genome scaffold as each amplicon marker (a total of 15 gene models  
203 including the candidate gene) were assessed for orthology with *C. elegans* genes where possible.  
204 Scaffolds containing the Hcms8a20 and *Hco-lgc-37* amplicon markers were small, so all gene models  
205 on each scaffold were assessed (1 and 6, respectively). A custom BLAST search (Liebert et al., 2000)  
206 (blastn -task dc-megablast -query H.contortus\_genes.fa -db C.elegans\_CDSs.fa -out outfile) was used  
207 to identify orthologues in the most current ensembl.org *C. elegans* CDS database downloaded at  
208 [ftp://ftp.ensembl.org/pub/release-83/fasta/caenorhabditis\\_elegans/cds/](ftp://ftp.ensembl.org/pub/release-83/fasta/caenorhabditis_elegans/cds/). Only unambiguous orthologues  
209 were used in the analysis of synteny. Identification of a *C. elegans* orthologue was considered  
210 unambiguous if the *H. contortus* query gene model identified a *C. elegans* gene model with an e-value  
211 of 1e-9 or less and with no other hits on different chromosomes having an e-value within one order of  
212 magnitude. *Hco-glc-5*, *Hco-avr-14* and *Hco-pgp-2* are located on chromosome 1, *Hco-lgc-37* on  
213 chromosome 3, and *Hco-dyf-7* on the X chromosome (Supplementary Table S2). A chromosomal  
214 assignment could not be made for *Hco-pgp-9* due to mixed chromosomal synteny with *C. elegans*  
215 orthologues, nor for Hcms8a20 due to the lack of adjacent gene models on the relatively short scaffold  
216 on which it was located (27 kb).

217 [Somewhere in section 2 mention which *P* value was considered significant because you  
218 mention *P* values in section 3.]

### 219 **3. Results**

220 *3.1. Amplicon markers for all the candidate loci show a high level of genetic differentiation between*  
221 *the H. contortus parental strains used in the two independent backcross experiments*

222 In order to investigate haplotype introgression between parental genomes during a serial  
223 backcross, markers with a high level of genetic differentiation between parental strains are needed. In

224 this particular case, haplotypes unique to the ivermectin-resistant parental strain, or those present at  
225 very different frequencies in the two parental strains, are the most informative for assessing haplotype  
226 introgression from each resistant parental strain into the backcross populations. Consequently, we first  
227 assessed the haplotype diversity of the seven amplicon markers within and among the parental strains  
228 used in the two backcrosses. We PCR-amplified and sequenced between 14 and 24 clones for each  
229 marker from the MHco3(ISE), MHco4(WRS) and MHco10(CAVR) parental strains (Table 1). A high  
230 level of sequence diversity was observed for all seven loci (Table 1). The mean number of haplotypes  
231 for the seven markers was 3.5, 8.33 and 5.83 haplotypes per locus for MHco3(ISE), MHco4(WRS) and  
232 MHco10(CAVR) parental strains, respectively (Table 1).

233         Although some shared haplotypes were present, the majority were not shared between the  
234 parental strains used in each backcross (Table 1). Pairwise  $F_{st}$  values were used to quantify the genetic  
235 differentiation for each amplicon marker between the parental strains (Table 2). There was a high level  
236 of genetic differentiation between the MHco3(ISE) susceptible parental strain and both resistant  
237 parental strains, MHco4(WRS) and MHco10(CAVR), for all seven amplicon markers. Pairwise  $F_{st}$   
238 values ranged between 0.078 and 0.533 and all were statistically significantly different from zero at  $P$   
239  $<0.01$  (Table 2).

240

241 *3.2. The amplicon marker adjacent to microsatellite Hmcs8a20 shows strong evidence of haplotype*  
242 *introgression from the ivermectin-resistant parental strain in both independent backcross populations*

243         We investigated the evidence for haplotype introgression from the resistant parental strains into  
244 the two independent backcross populations for an amplicon marker adjacent to microsatellite  
245 Hmcs8a20. This marker was PCR-amplified, cloned and sequenced from the MHco3/4.BC and  
246 MHco3/10.BC backcross populations and the haplotype profiles compared with those of the parental

247 strains (Table 1). In both of these backcross populations, this marker showed a high degree of genetic  
248 differentiation from the MHco3(ISE) susceptible parental strain;  $F_{st}$  values were high and statistically  
249 significantly different from zero for both the MHco3(ISE) - MHco3/4.BC and MHco3(ISE) -  
250 MHco3/10.BC pairwise comparisons ( $F_{st} = 0.383$ ,  $P = 0.000$  and  $F_{st} = 0.512$ ,  $P = 0.000$ , respectively)  
251 (Table 3). The most frequent haplotypes of this marker in the two backcross populations were  
252 haplotype-D in MHco3/4.BC and haplotype-E in MHco3/10.BC at 60.9% and 78.3% frequencies,  
253 respectively. These haplotypes were not detected in the MHco3(ISE) susceptible parental isolate but  
254 were present in respective resistant parental strains used in each backcross (Fig. 1). These results  
255 suggest haplotype introgression from each resistant parental strain into the MHco3(ISE) susceptible  
256 parental background during both independent backcrossing experiments.

257

258 *3.3. The amplicon markers within the Hco-glc-5, Hco-avr-14, Hco-pgp-9 and Hco-dyf-7 genes show no*  
259 *evidence of haplotype introgression from the ivermectin-resistant parental strain in either of the*  
260 *independent backcross populations*

261 Amplicon markers within the *Hco-glc-5*, *Hco-avr-14*, *Hco-pgp-9* and *Hco-dyf-7* genes were  
262 PCR-amplified, cloned and sequenced from the MHco3/4.BC and MHco3/10.BC backcross  
263 populations, and the haplotype profiles compared with those present in the parental strains (Table 1).  
264 We measured the level of pairwise genetic differentiation for each of these markers between the  
265 MHco3(ISE) parental strain and each of the MHco3/4.BC and MHco3/10.BC backcross populations. In  
266 all pairwise comparisons, the  $F_{st}$  values were not statistically significantly different from zero (Table  
267 3). In contrast to the Hcms8a20 amplicon marker, the most frequent haplotype present in each  
268 backcross population was not unique to the resistant parental strain for any of the four candidate  
269 ivermectin resistance loci. Furthermore, in all cases, the most frequent haplotype present in backcross

270 populations was present at a higher frequency in the MHco3(ISE) susceptible parental strain than the  
271 resistant parental strain (Figs. 2, 3). These results suggest no evidence of haplotype introgression from  
272 either resistant parental strain into the MHco3(ISE) susceptible parental background during either of  
273 the backcrossing experiments for these four amplicon markers.

274

275 *3.4. The amplicon markers within the Hco-lgc-37 and Hco-pgp-2 genes show weak evidence of*  
276 *haplotype introgression from the ivermectin-resistant parental strain in the MHco3/4.BC backcross but*  
277 *not the MHco3/10.BC backcross populations*

278 Amplicon markers within the *Hco-lgc-37* and *Hco-pgp-2* genes were PCR-amplified, cloned  
279 and sequenced from the MHco3/4.BC and MHco3/10.BC backcross populations and the haplotype  
280 profiles compared with those present in the parental strains (Table 1). We measured the level of  
281 pairwise genetic differentiation for each of these markers between the MHco3(ISE) parental strain and  
282 each of the MHco3/4.BC and MHco3/10.BC backcross populations. In the case of the MHco3/10.BC  
283 backcross, the  $F_{st}$  values were not statistically significantly different from zero for either marker (Table  
284 3). For the MHco3/4.BC backcross, the MHco3(ISE)-MHco3/4.BC pairwise  $F_{st}$  values were  
285 statistically significantly different from zero for both the *Hco-lgc-37* and *Hco-pgp-2* markers at 0.220  
286 ( $P = 0.004$ ) and 0.115 ( $P = 0.000$ ), respectively (Table 3). For these two pairwise comparisons, there  
287 was also a haplotype present in the backcross populations that was unique to the resistant parental  
288 strain with respect to the MHco3(ISE) parental strain; haplotype-I of *Hco-pgp-2* and haplotype-H of  
289 *Hco-lgc-37* (Fig. 2). However, these were only present at very low frequencies in each backcross (Fig.  
290 2). These results provide weak evidence for haplotype introgression from the resistant parental strains  
291 into the MHco3(ISE) susceptible parental background for these two markers in the MHco3/4.BC  
292 backcross but not in the MHco3/10.BC backcross populations.

293

#### 294 **4. Discussion**

295           The objective of this work was to investigate a number of leading candidate loci for evidence of  
296 genetic linkage to a major ivermectin resistance locus in two ivermectin-resistant *H. contortus* strains;  
297 MHco4(WRS) and MHco10(CAVR). These two strains have previously been serially backcrossed  
298 against the ivermectin-susceptible *H. contortus* genome reference strain MHco3(ISE) with ivermectin  
299 selection applied at each generation (Redman et al., 2012). The resulting fourth generation backcross  
300 populations (MHco3/4.BC and MHco3/10.BC) have been previously genetically and phenotypically  
301 validated (Redman et al., 2012). In that study, 17 out of 18 microsatellite markers were found to have  
302 allelic profiles in the MHco3/4.BC and MHco3/10.BC populations that were similar to those of the  
303 MHco3(ISE) susceptible parental strain. This demonstrated that the genetic background of these  
304 backcross populations was predominantly derived from the MHco3(ISE) susceptible parental strain as  
305 expected from the serial backcrossing regime. In the original published study, just one of the 18  
306 microsatellite markers, Hcms8a20, had an allele at high frequency in the backcross populations  
307 (following ivermectin treatment) that was derived from the resistant parental strains in both serial  
308 backcross experiments (Redman et al., 2012). This result suggested that this microsatellite marker is  
309 linked to an important ivermectin resistance locus in both the MHco4(WRS) and MHco10(CAVR)  
310 ivermectin-resistant strains.

311           In the work presented here, we aimed to test the hypothesis that the Hcms8a20 microsatellite  
312 marker was linked to an important ivermectin-resistant locus in the MHoc4(WRS) and  
313 MHco10(CAVR) strains and, at the same time, test the other leading candidate ivermectin resistance  
314 loci from the peer-reviewed literature. Fig. 4 illustrates the conceptual approach we adopted. We  
315 examined the haplotype profiles of PCR amplicon markers located within, or close to, our loci of

316 interest in the parental and backcross populations of both serial backcross experiments. If a genetic  
317 marker is closely linked to an important ivermectin resistance locus, haplotypes of that marker that are  
318 present in the ivermectin-resistant parental strain, and linked to the ivermectin resistance mutation,  
319 should be inherited through the backcross due to the ivermectin selection applied at each generation by  
320 so called “genetic hitchhiking” (Fig. 4A). Consequently, such haplotypes will be introgressed from the  
321 ivermectin-resistant parental strain into the predominantly MHco3(ISE) genetic background during the  
322 backcrossing procedure (Fig. 4A). Hence, it is possible to make predictions regarding the haplotype  
323 profiles of markers in the backcross populations depending on whether or not they are linked to an  
324 important ivermectin resistance mutation (Fig. 4B). The presence and frequency of haplotypes for a  
325 marker that is not linked to an important ivermectin resistance locus should be very similar to those  
326 found in the MHco3(ISE) parental strain and haplotypes that are unique to the resistant parental strain  
327 should be absent (or rare) in the backcross populations. This is because there will be no introgression of  
328 haplotypes from the ivermectin-resistant parental strain into the backcross populations in that region of  
329 the genome (markers A and C in Fig. 4). Conversely, the presence and frequency of haplotypes for a  
330 marker that is linked to an important ivermectin resistance locus should differ significantly from those  
331 in the MHco3(ISE) parental strain due to the presence of one or more haplotypes that have been  
332 introgressed from the resistant parental strain (markers B and D in Fig. 4). The extent of this difference  
333 will depend on how closely linked the marker is to the loci under selection.

334           The haplotype profiles of the amplicon marker located 17.8 kb away from the Hcms8a20  
335 microsatellite marker locus clearly fit the predictions for a marker linked to an important ivermectin  
336 resistance locus. In both the MHco3/4.BC and MHco3/10.BC backcross populations, the haplotype  
337 profiles of the Hcms8a20 amplicon marker were significantly different to the haplotype profile that was  
338 present in the MHco3(ISE) susceptible reference strain (Table 3, Fig. 1). This is indicated by the high  
339  $F_{st}$  values observed between both backcross populations and the MHco3(ISE) strain, by far the highest

340 values for any of the seven loci examined (Table 3). Furthermore, in both backcross populations the  
341 most frequent haplotype for the Hcms8a20 amplicon marker was one which was present in each  
342 ivermectin-resistant parental strain but absent from the MHco3(ISE) susceptible parental strain;  
343 haplotype-D in MHco3/4.BC and haplotype-E in MHco3/10.BC (Fig. 1). This suggests that these  
344 haplotypes have been inherited from the resistant parental strains during the serial backcrosses under  
345 the influence of the ivermectin selection applied at each generation. Interestingly, a different haplotype  
346 has been introgressed from each resistant parental strain in the two independent backcross experiments.  
347 This is consistent with the previously published results using the allele profiles of the Hcms8a20  
348 microsatellite marker itself (Redman et al., 2012). In that case, for each separate backcross experiment,  
349 a different microsatellite allele, specific to each ivermectin-resistant parental strain, was introgressed  
350 into the backcross populations. This is not necessarily surprising since MHco4(WRS) and  
351 MHco10(CAVR) were originally derived from different continents - South Africa and Australia,  
352 respectively - so the causal ivermectin resistance mutation(s) may well have originated independently  
353 in the two strains. In that case, they would be expected to be present on different haplotype  
354 backgrounds in each strain.

355 In contrast to the Hcms8a20 marker, the haplotype profiles of the amplicon markers within the  
356 candidate ivermectin resistance genes *Hco-glc-5*, *Hco-avr-14*, *Hco-pgp-9* and *Hco-dyf-7* clearly fit the  
357 predictions for markers that are not linked to an important ivermectin resistance locus in the  
358 MHco4(WRS) and MHco10(CAVR) resistant strains. For these markers, there was no significant  
359 difference in the haplotypes present in either of the independent backcross populations compared with  
360 the susceptible MHco3(ISE) population. Furthermore, unlike for the Hcms8a20 amplicon marker, there  
361 were no haplotypes unique to either resistant parental strain present in either of the backcross  
362 populations for any of these genes. This was also the case for the amplicon markers within the *Hco-lgc-*  
363 *37* and *Hco-pgp-2* genes for the MHco3/10.BC backcross population, suggesting these genes are also

364 not linked to an important ivermectin resistance locus in the MHco10(CAVR) strain. However, the  
365 result for these two markers was less clear cut in the other backcross experiment; there was a  
366 statistically significant difference in the haplotypes present in the MHco3/4.BC backcross population  
367 compared with the susceptible MHco3(ISE) population. Also, for each of these two markers, there was  
368 a haplotype present in the MHco3/4.BC backcross population that was unique to the MHco4(WRS)  
369 resistant parental strain (haplotype-I for *Hco-pgp-2* and haplotype-H for *Hco-lgc-37*). However, these  
370 haplotypes were present at very low frequencies in the MHco3/4.BC population. Overall, we conclude  
371 there is weak but inconclusive evidence of linkage of the *Hco-lgc-37* and *Hco-pgp-2* genes to an  
372 important ivermectin resistance locus in the MHco4(WRS), but not the MHco10(CAVR), strain. This  
373 more ambiguous result could potentially be due to these genes being distantly linked to an important  
374 ivermectin resistance locus on the same chromosome or tightly linked to a locus with a minor effect.

375         Although the results presented here provide additional evidence that the Hcms8a20 marker is  
376 genetically linked to an important ivermectin resistance locus in the MHco4(WRS) and  
377 MHco10(CAVR) strains, this is not the case for the other leading candidate ivermectin resistance loci.  
378 It is possible that these loci are not associated with ivermectin resistance given they have been  
379 implicated largely on the basis of single studies using a small number of populations and often a small  
380 number of individuals within each population. Other recent work has also found no evidence of  
381 selection for the *Hco-lgc-37*, *Hco-glc-5*, *Hco-avr-14* and *Hco-dyf-7* loci when comparing *H. contortus*  
382 from UK farms with a history of ivermectin treatment with those without (Laing R, Maitland K,  
383 Lecová L, Skuce P, Tait A, Devaney E; In press [either 'in press' or 'unpublished data']).  
384 Alternatively, it may be that these loci are linked to an important ivermectin loci in some strains but not  
385 in MHco4(WRS) and MHco10(CAVR). This is possible since the previous published work implicating  
386 these candidate loci was not conducted on these particular strains.

387           Although this and previous work provides strong evidence that the Hcms8a20 microsatellite  
388 marker is genetically linked to an important ivermectin resistance locus in the MHco4(WRS) and  
389 MHco10(CAVR) strains, it could be still be relatively distant from the causal mutation(s). Only limited  
390 genetic recombination will have occurred in four generations of backcrossing. Consequently, the  
391 genomic region(s) introgressed into the backcross populations from the resistant parental strains is  
392 expected to be large. This is supported by recent genome-wide SNP analysis of the backcross and  
393 parental populations that has identified several genomic scaffolds that have a strong signal of  
394 introgression, some of which are several Mb in length (Martinelli, A, Rezansoff, A, Doyle, S, Gilleard,  
395 J and Cotton, J, unpublished data). The Hcms8a20 marker is located on one of these scaffolds,  
396 providing further support for its linkage to an important ivermectin resistance locus (Martinelli, A,  
397 Rezansoff, A, Doyle, S, Gilleard, J and Cotton, J, unpublished data). Further interrogation of the *H.*  
398 *contortus* MHco3(ISE) reference genome as the assembly improves will help locate the genomic  
399 position of the causal mutations to which the Hcms8a20 locus is linked ([http://www.sanger.ac.uk/  
400 resources/downloads/helminths/haemonchus-contortus.html](http://www.sanger.ac.uk/resources/downloads/helminths/haemonchus-contortus.html)).

401

## 402 **Acknowledgements**

403           We are grateful for funding from the Canadian Institutes of Health Research (CIHR) grant  
404 230927 and to the NSERC-CREATE Host Pathogen Interactions (HPI) graduate training program at  
405 the University of Calgary, Canada. RL acknowledges funding from the Scottish Government through  
406 the Strategic Partnership for Animal Science Excellence (SPASE) and BBRSC Strategic Lola grant  
407 (BB/M003949/1). We also thank Libby Redman for access to samples and Umer Chaudhry and Susan  
408 Stasiuk for guidance with laboratory techniques and protocols.

409



411 **References**

412

413 Bartley, D.J., McAllister, H., Bartley, Y., Dupuy, J., Ménez, C., Alvinerie, M., Jackson, F., Lespine, A.,  
414 2009. P-glycoprotein interfering agents potentiate ivermectin susceptibility in ivermectin sensitive  
415 and resistant isolates of *Teladorsagia circumcincta* and *Haemonchus contortus*. *Parasitology* 136,  
416 1081–8. doi:10.1017/S0031182009990345

417 Beech, R., Levitt, N., Cambos, M., Zhou, S., Forrester, S.G., 2010. Association of ion-channel  
418 genotype and macrocyclic lactone sensitivity traits in *Haemonchus contortus*. *Mol. Biochem.*  
419 *Parasitol.* 171, 74–80. doi:10.1016/j.molbiopara.2010.02.004

420 Beech, R.N., Skuce, P., Bartley, D.J., Martin, R.J., Prichard, R.K., Gilleard, J.S., 2011. Anthelmintic  
421 resistance: markers for resistance, or susceptibility? *Parasitology* 138, 160–174.  
422 doi:10.1017/S0031182010001198

423 Beech, R.N., Wolstenholme, A.J., Neveu, C., Dent, J.A., 2010. Nematode parasite genes: what's in a  
424 name? *Trends Parasitol.* 26, 334–340. doi:10.1016/j.pt.2010.04.003

425 Blackhall, W.J., Liu, H.Y., Xu, M., Prichard, R.K., Beech, R.N., 1998. Selection at a P-glycoprotein  
426 gene in ivermectin- and moxidectin-selected strains of *Haemonchus contortus*. *Mol. Biochem.*  
427 *Parasitol.* 95, 193–201. doi:10.1016/S0166-6851(98)00087-5

428 Blackhall, W.J., Prichard, R.K., Beech, R.N., 2003. Selection at a  $\gamma$ -aminobutyric acid receptor gene in  
429 *Haemonchus contortus* resistant to avermectins/milbemycins. *Mol. Biochem. Parasitol.* 131, 137–  
430 145. doi:10.1016/S0166-6851(03)00201-9

431 Blackhall, W.J., Prichard, R.K., Beech, R.N., 1998. *Haemonchus contortus*: Selection at a Glutamate-  
432 Gated Chloride Channel. *Exp. Parasitol.* 48, 42–48.

433 Chaudhry, U., Redman, E.M., Raman, M., Gilleard, J.S., 2015. Genetic evidence for the spread of a  
434 benzimidazole resistance mutation across southern India from a single origin in the parasitic  
435 nematode *Haemonchus contortus*. *Int. J. Parasitol.* 45, 721–728. doi:10.1016/j.ijpara.2015.04.007

436 Dent, J.A., Smith, M.M., Vassilatis, D.K., Avery, L., 2000. The genetics of ivermectin resistance in  
437 *Caenorhabditis elegans*. *Proc. Natl. Acad. Sci. U. S. A.* 97, 2674–2679.  
438 doi:10.1073/pnas.97.6.2674

- 439 Edgar, R.C., 2004. MUSCLE: multiple sequence alignment with high accuracy and high throughput.  
440 Nucleic Acid Res. 32, 1792–1797. doi:10.1093/nar/gkh340
- 441 Excoffier, L., Laval, G., Schneider, S., 2005. Arlequin (version 3.0): an integrated software package for  
442 population genetics data analysis. Evol Bioinform Online 1, 47–50. doi:10.1111/j.1755-  
443 0998.2010.02847.x
- 444 Ghosh, R., Andersen, E.C., Shapiro, J. a., Gerke, J.P., Kruglyak, L., 2012. Natural Variation in a  
445 Chloride Channel Subunit Confers Avermectin Resistance in *C. elegans*. Science. 335(6068),  
446 574–578. doi:10.1126/science.1214318
- 447 Gilleard, J.S., 2013. *Haemonchus contortus* as a paradigm and model to study anthelmintic drug  
448 resistance. Parasitology 140, 1506–1522. doi:10.1017/S0031182013001145
- 449 Gilleard, J.S., 2006. Understanding anthelmintic resistance: The need for genomics and genetics. Int. J.  
450 Parasitol. 36, 1227–1239. doi:10.1016/j.ijpara.2006.06.010
- 451 Gilleard, J.S., Beech, R.N., 2007. Population genetics of anthelmintic resistance in parasitic nematodes.  
452 Parasitology 134, 1133–1147. doi:10.1017/S0031182007000066
- 453 Glendinning, S.K., Buckingham, S.D., Sattelle, D.B., Wonnacott, S., Wolstenholme, A.J., 2011.  
454 Glutamate-Gated Chloride Channels of *Haemonchus contortus* Restore Drug Sensitivity to  
455 Ivermectin Resistant *Caenorhabditis elegans*. PLoS One 6, e22390.  
456 doi:10.1371/journal.pone.0022390
- 457 Heiman, M.G., Shaham, S., 2009. DEX-1 and DYF-7 Establish Sensory Dendrite Length by Anchoring  
458 Dendritic Tips during Cell Migration. Cell 137, 344–355. doi:10.1016/j.cell.2009.01.057
- 459 Jagannathan, S., Laughton, D.L., Critten, C.L., Skinner, T.M., Horoszok, L., Wolstenholme, A.J., 1999.  
460 Ligand-gated chloride channel subunits encoded by the *Haemonchus contortus* and *Ascaris suum*  
461 orthologues of the *Caenorhabditis elegans* gbr-2 (avr-14) gene. Mol. Biochem. Parasitol. 103,  
462 129–140. doi:10.1016/S0166-6851(99)00120-6
- 463 James, C.E., Hudson, A.L., Davey, M.W., 2009. Drug resistance mechanisms in helminths: is it  
464 survival of the fittest? Trends Parasitol. 25, 328–335. doi:10.1016/j.pt.2009.04.004
- 465 Kaplan, R.M., Vidyashankar, A.N., 2012. An inconvenient truth: Global worming and anthelmintic  
466 resistance. Vet. Parasitol. 186, 70–78. doi:10.1016/j.vetpar.2011.11.048

- 467 Kearse, M., Moir, R., Wilson, A., Stones-Havas, S., Cheung, M., Sturrock, S., Buxton, S., Cooper, A.,  
468 Markowitz, S., Duran, C., Thierer, T., Ashton, B., Meintjes, P., Drummond, A., 2012. Geneious  
469 Basic: an integrated and extendable desktop software platform for the organization and analysis of  
470 sequence data. *Bioinformatics* 28, 1647–1649. doi:10.1093/bioinformatics/bts199
- 471 Laing, R., Hunt, M., Protasio, A. V, Saunders, G., Mungall, K., Laing, S., Jackson, F., Quail, M.,  
472 Beech, R., Berriman, M., Gilleard, J.S., 2011. Annotation of two large contiguous regions from  
473 the *Haemonchus contortus* genome using RNA-seq and comparative analysis with *Caenorhabditis*  
474 *elegans*. *PLoS One* 6, e23216. doi:10.1371/journal.pone.0023216
- 475 Laing, R., Kikuchi, T., Martinelli, A., Tsai, I., Beech, R., Redman, E., Holroyd, N., Bartley, D.,  
476 Beasley, H., Britton, C., Curran, D., Devaney, E., Gilabert, A., Hunt, M., Jackson, F., Johnston, S.,  
477 Kryukov, I., Li, K., Morrison, A., Reid, A., Sargison, N., Saunders, G., Wasmuth, J.,  
478 Wolstenholme, A., Berriman, M., Gilleard, J., Cotton, J., 2013. The genome and transcriptome of  
479 *Haemonchus contortus*, a key model parasite for drug and vaccine discovery. *Genome Biol.* 14,  
480 R88. doi:10.1186/gb-2013-14-8-r88
- 481 Le Jambre, L., Gill, J., Lenane, I., Lacey, E., 1995. Characterization of an avermectin resistant strain of  
482 australian *Haemonchus contortus*. *Int. J. Parasitol.* 25, 691–698.
- 483 Le Jambre, L.F., Lenane, I.J., Wardrop, A.J., 1999. A hybridisation technique to identify anthelmintic  
484 resistance genes in *Haemonchus*. *Int. J. Parasitol.* 29, 1979–1985. doi:10.1016/S0020-  
485 7519(99)00157-5
- 486 Liebert, M.A., Zhang, Z., Schwartz, S., Wagner, L., Miller, W., 2000. A Greedy Algorithm for  
487 Aligning DNA Sequences 7, 203–214. [journal title msising?]
- 488 McCavera, S., Rogers, A.T., Yates, D.M., Woods, D.J., Wolstenholme, A.J., 2009. An ivermectin-  
489 sensitive glutamate-gated chloride channel from the parasitic nematode *Haemonchus contortus*.  
490 *Mol Pharm* 75, 1347–1355. doi:10.1124/mol.108.053363.living
- 491 McCavera, S., Walsh, T.K., Wolstenholme, A.J., 2007. Nematode ligand-gated chloride channels: an  
492 appraisal of their involvement in macrocyclic lactone resistance and prospects for developing  
493 molecular markers. *Parasitology* 134, 1111–1121. doi:10.1017/S0031182007000042
- 494 Redman, E., Packard, E., Grillo, V., Smith, J., Jackson, F., Gilleard, J.S., 2008. Microsatellite analysis

495 reveals marked genetic differentiation between *Haemonchus contortus* laboratory isolates and  
496 provides a rapid system of genetic fingerprinting. *Int. J. Parasitol.* 38, 111–122.  
497 doi:10.1016/j.ijpara.2007.06.008

498 Redman, E., Sargison, N., Whitelaw, F., Jackson, F., Morrison, A., Bartley, D.J., Gilleard, J.S., 2012.  
499 Introgression of Ivermectin Resistance Genes into a Susceptible *Haemonchus contortus* Strain by  
500 Multiple Backcrossing. *PLoS Pathog.* 8, e1002534. doi:10.1371/journal.ppat.1002534

501 Redman, E., Whitelaw, F., Tait, A., Burgess, C., Bartley, Y., Skuce, P.J., Jackson, F., Gilleard, J.S.,  
502 2015. The emergence of resistance to the benzimidazole anthelmintics in parasitic nematodes of  
503 livestock is characterised by multiple independent hard and soft selective sweeps. *PLoS Negl.*  
504 *Trop. Dis.* 9, e0003494. doi:10.1371/journal.pntd.0003494

505 Roos, M.H., Otsen, M., Hoekstra, R., Veenstra, J.G., Lenstra, J.A., 2004. Genetic analysis of  
506 inbreeding of two strains of the parasitic nematode *Haemonchus contortus*. *Int. J. Parasitol.* 34,  
507 109–115. doi:10.1016/j.ijpara.2003.10.002

508 Sangster, N.C., Bannan, S.C., Weiss, a S., Nulf, S.C., Klein, R.D., Geary, T.G., 1999. *Haemonchus*  
509 *contortus*: sequence heterogeneity of internucleotide binding domains from P-glycoproteins. *Exp.*  
510 *Parasitol.* 91, 250–257. doi:S0014489498943739 [pii]

511 Schinkel, A.H., 1999. P-Glycoprotein, a gatekeeper in the blood-brain barrier. *Adv. Drug Deliv. Rev.*  
512 36, 179–194. doi:10.1016/S0169-409X(98)00085-4

513 Urdaneta-Marquez, L., Bae, S.H., Janukavicius, P., Beech, R., Dent, J., Prichard, R., 2014. A dyf-7  
514 haplotype causes sensory neuron defects and is associated with macrocyclic lactone resistance  
515 worldwide in the nematode parasite *Haemonchus contortus*. *Int. J. Parasitol.* 44, 1063–1071.  
516 doi:10.1016/j.ijpara.2014.08.005

517 Van Wyk, J.A., Malan, F.S., 1988. Resistance of field strains of *Haemonchus contortus* to ivermectin,  
518 closantel, rafoxanide and the benzimidazoles in South Africa. *Vet. Rec.* 123, 226–228.  
519 doi:10.1136/vr.123.9.226

520 Williamson, S.M., Wolstenholme, a J., 2012. P-glycoproteins of *Haemonchus contortus*: development  
521 of real-time PCR assays for gene expression studies. *J. Helminthol.* 86, 202–208.  
522 doi:10.1017/S0022149X11000216

523 Wolstenholme, a J., Rogers, a T., 2005. Glutamate-gated chloride channels and the mode of action of  
524 the avermectin/milbemycin anthelmintics. *Parasitology* 131 Suppl, S85–S95.  
525 doi:10.1017/S0031182005008218

526 Xu, M., Molento, M., Blackhall, W., Ribeiro, P., Beech, R., Prichard, R., 1998. Ivermectin resistance in  
527 nematodes may be caused by alteration of P-glycoprotein homolog. *Mol. Biochem. Parasitol.* 91,  
528 327–335. doi:10.1016/S0166-6851(97)00215-6

529

530

531

532 **Figure Legends**

533 [Each figure legend must 'stand alone', separate from every other figure legend and the main text.  
534 Therefore if the information provided in the figure legend is specific to a particular parasite  
535 genus/species, the genus/species should be mentioned in the first summary sentence of the figure  
536 legend.]

537

538 **Fig. 1.** Frequency histograms of haplotypes of the amplicon marker adjacent to microsatellite  
539 Hcms8a20. Haplotypes are labelled alphabetically on the X axis with respective frequencies observed  
540 on the Y axis in each population. (A) Haplotype distributions for the MHco4(WRS) x MHco3(ISE)  
541 backcross by frequency histograms for MHco3(ISE), MHco4(WRS) and MHco3/4.BC, respectively.  
542 (B) Haplotype distributions for the MHco10(CAVR) x MHco3(ISE) backcross by frequency  
543 histograms for MHco3(ISE), MHco10(CAVR) and MHco3/10.BC, respectively.

544

545 **Fig. 2.** Haplotype distributions for the candidate loci in the MHco4(WRS) x MHco3(ISE) backcross.  
546 Frequency histograms of haplotypes of the six candidate gene loci assessed in this study are shown for  
547 the MHco3(ISE), MHco4(WRS) and MHco3/4.BC backcross strains. Haplotypes are labelled  
548 alphabetically on the X axis with respective frequencies observed on the Y axis in each population.

549

550 **Fig. 3.** Haplotype distributions for the candidate loci in the MHco10(CAVR) x MHco3(ISE) backcross.  
551 Frequency histograms of haplotypes of the six candidate gene loci assessed in this study are shown for  
552 the MHco3(ISE), MHco10(CAVR) and MHco3/10.BC backcross strains. Haplotypes are labelled  
553 alphabetically on the X axis with respective frequencies observed on the Y axis in each population.

554

555 **Fig. 4.** [?general heading] (A) Schematic representation of the genomes of the resistant and susceptible  
556 parental strains and the backcross population. The coloured bars represent the five pairs of  
557 chromosomes with the resistant parental strain genetic background represented in red and the  
558 susceptible parental genetic background represented in blue. Causal resistance mutations are indicated  
559 by \*. The positions of four hypothetical genetic markers A, B, C and D are indicated. (B) Predictions  
560 for the haplotype profiles of the four hypothetical genetic markers in the backcross population.

561

562

563

564

565 [For both supplementary figures, given the larges amounts of data (Alex Loukas has approved this  
566 requested change), please consider submitting the data to Mendeley and replace all references to the  
567 figures in the manuscript with the relevant urls supplied by Mendeley. See <https://data.mendeley.com/>]

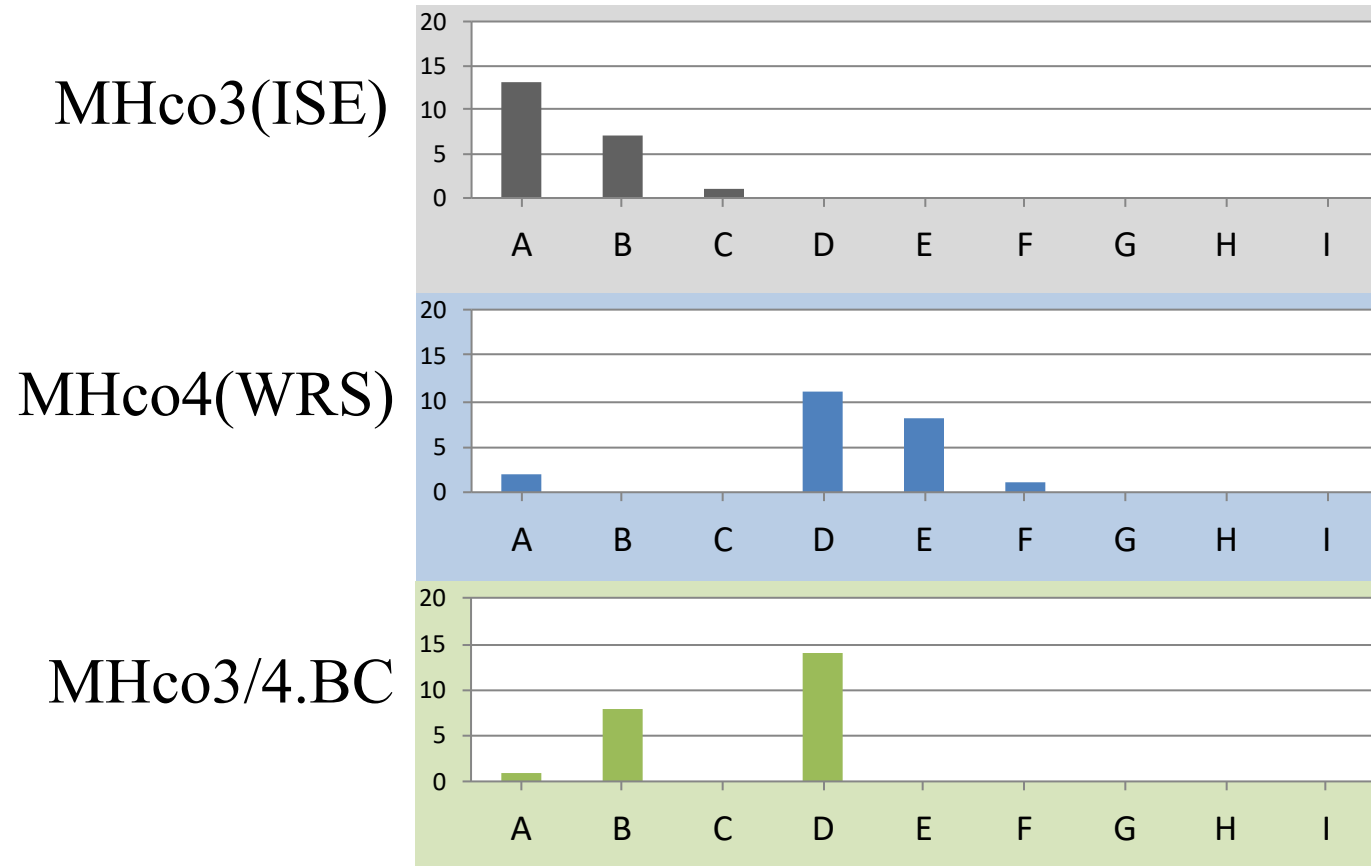
568

569 **Supplementary Fig. S1.** Sequence alignments for each of the seven loci using unedited sequences (no  
570 singleton single nucleotide polymorphisms (SNPs) removed).

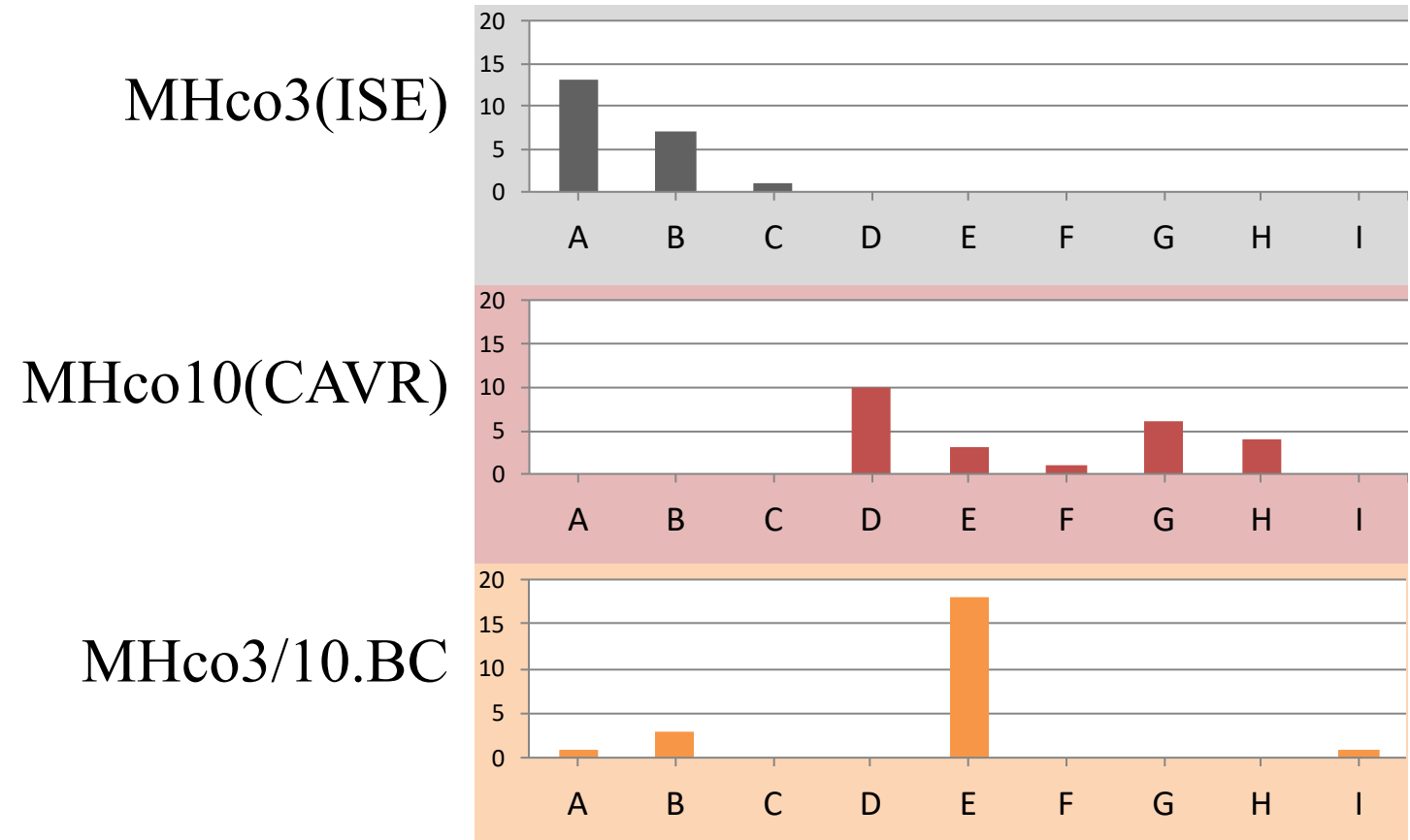
571

572 **Supplementary Fig. S2.** Sequence alignments for each of the seven loci using edited sequences  
573 (singleton single nucleotide polymorphisms (SNPs) removed).

Panel A



Panel B

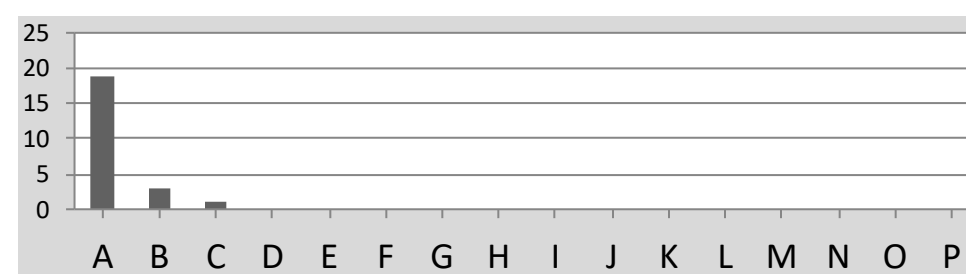


*Hco-glc-5*

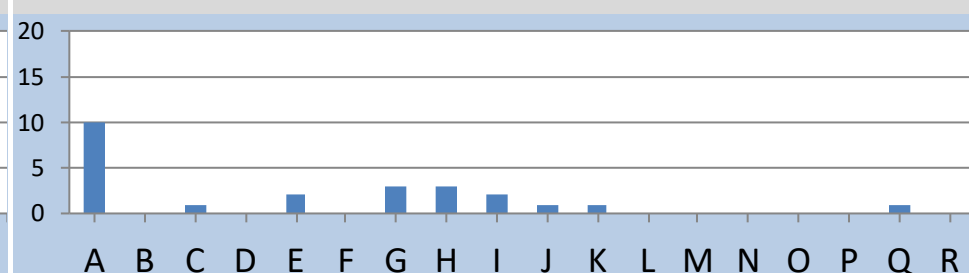
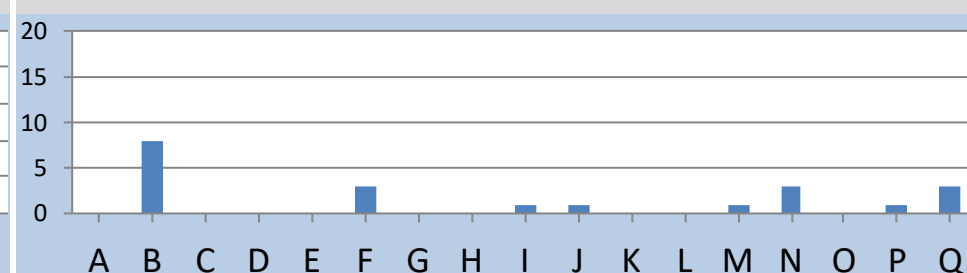
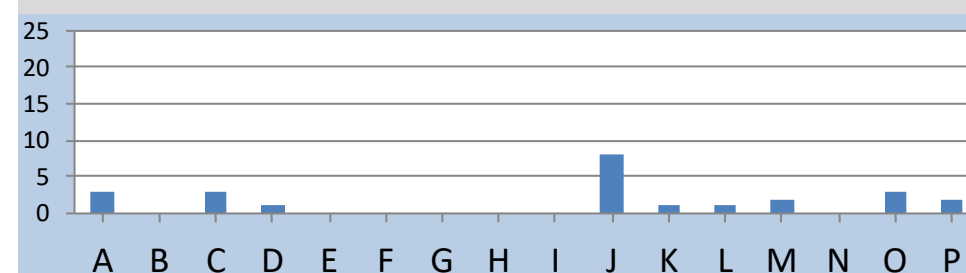
*Hco-avr-14*

*Hco-lgc-37*

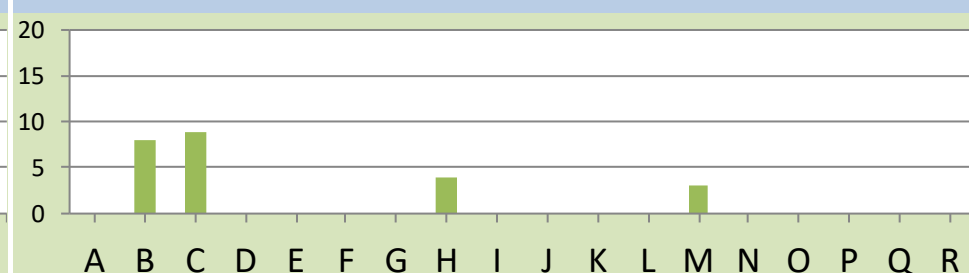
MHco3(ISE)



MHco4(WRS)



MHco3/4.BC

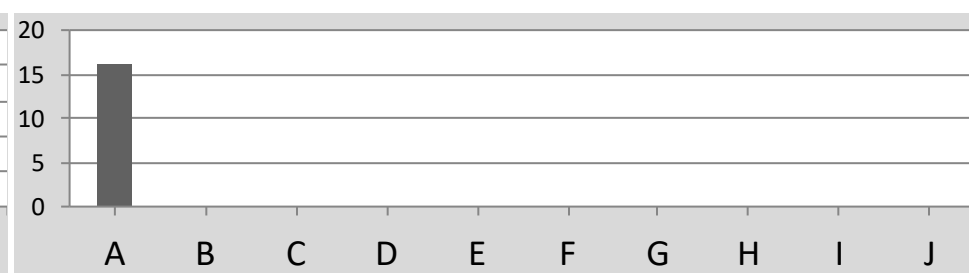
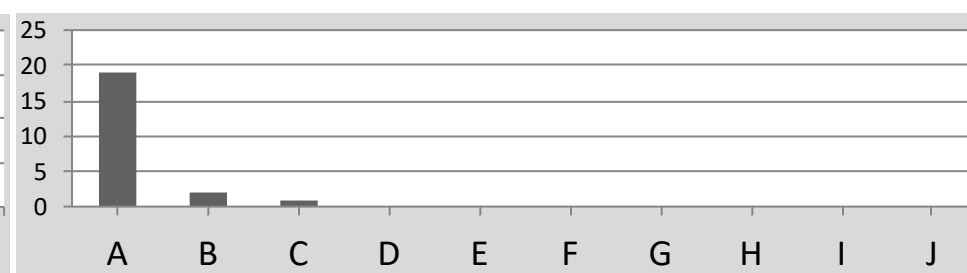
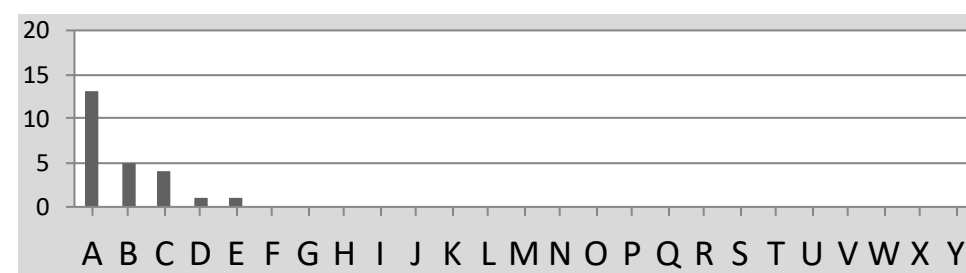


*Hco-pgp-9*

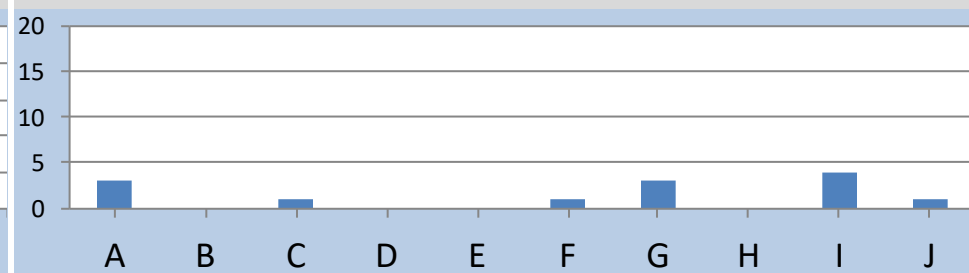
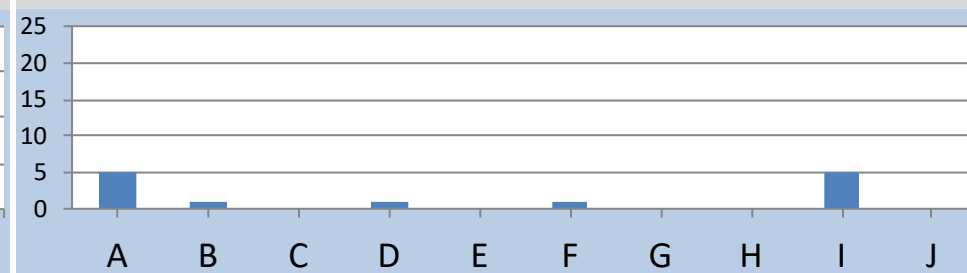
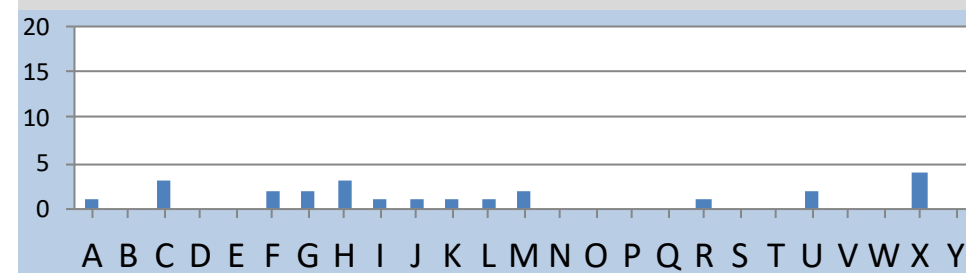
*Hco-pgp-2*

*Hco-dyf-7*

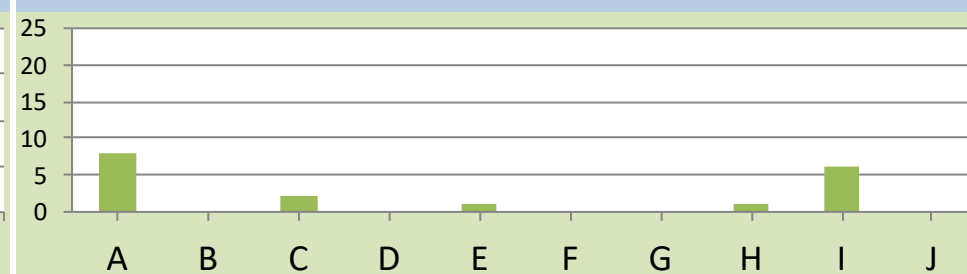
MHco3(ISE)



MHco4(WRS)



MHco3/4.BC

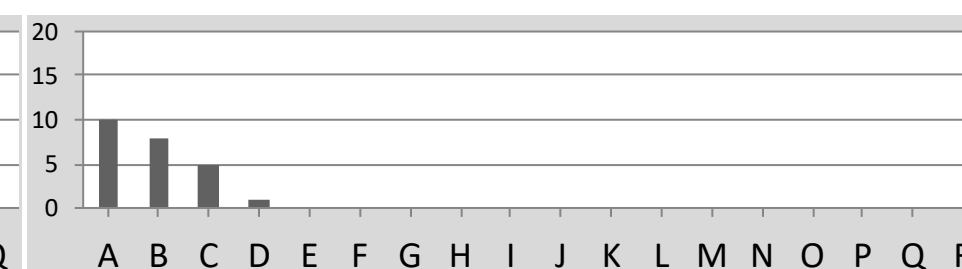
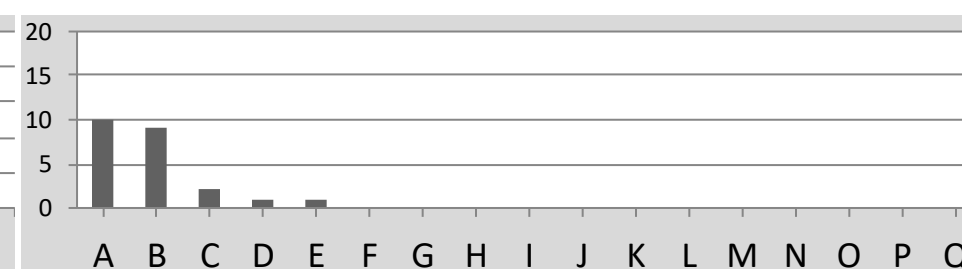
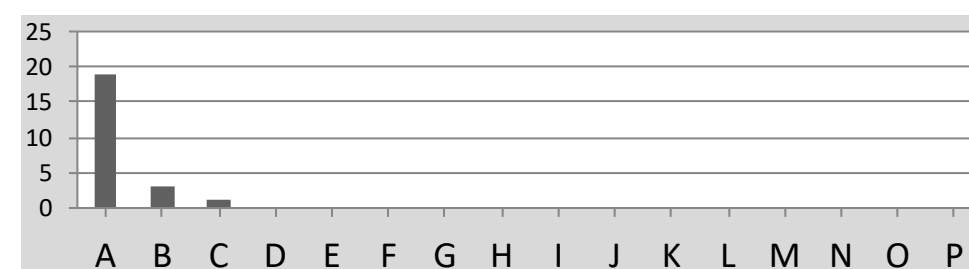


*Hco-glc-5*

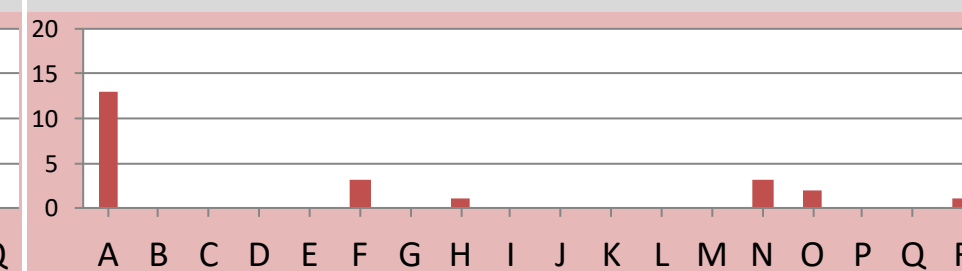
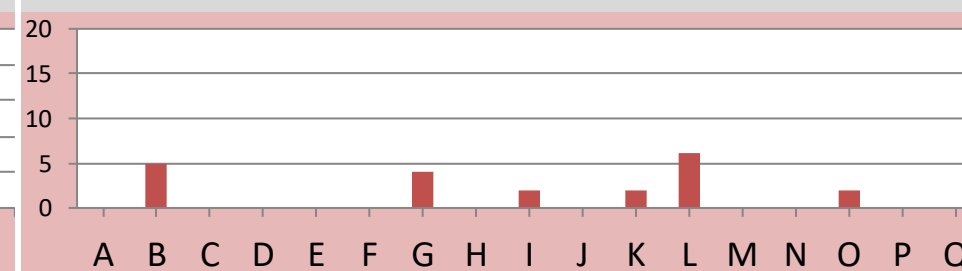
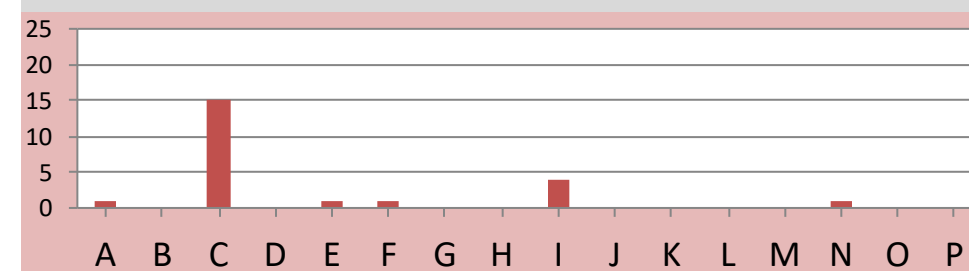
*Hco-avr-14*

*Hco-lgc-37*

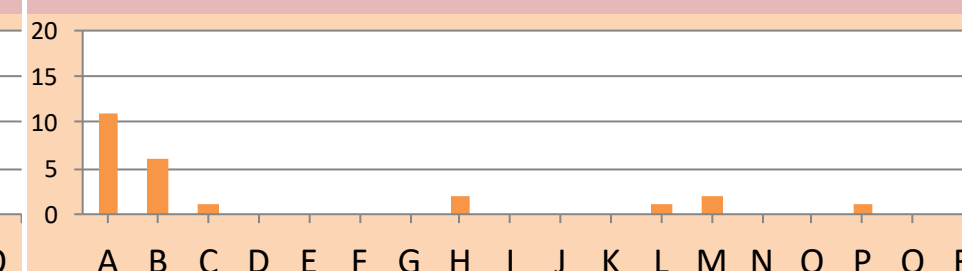
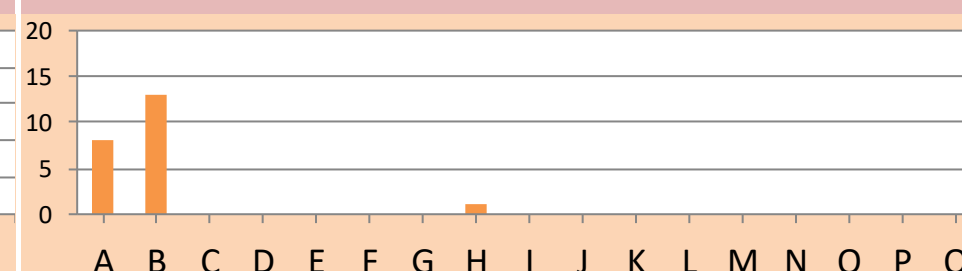
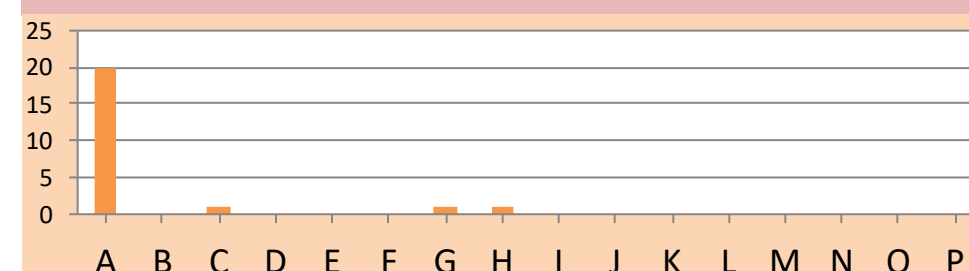
MHco3(ISE)



MHco10(CAVR)



MHco3/10.BC

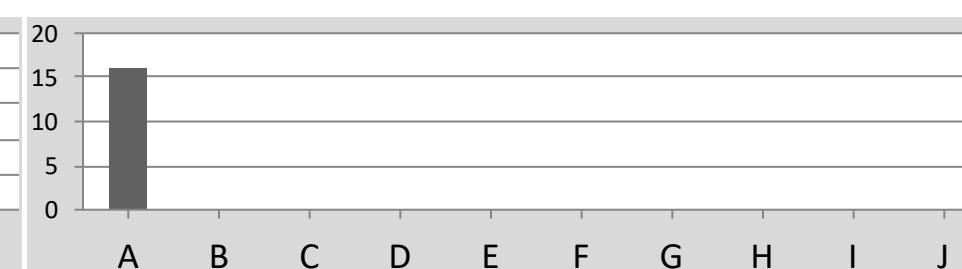


*Hco-pgp-9*

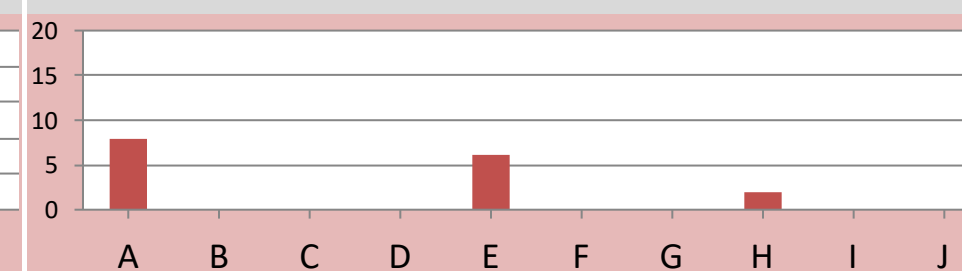
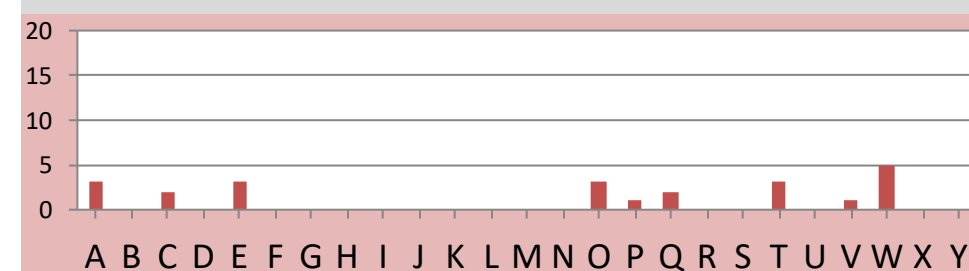
*Hco-pgp-2*

*Hco-dyf-7*

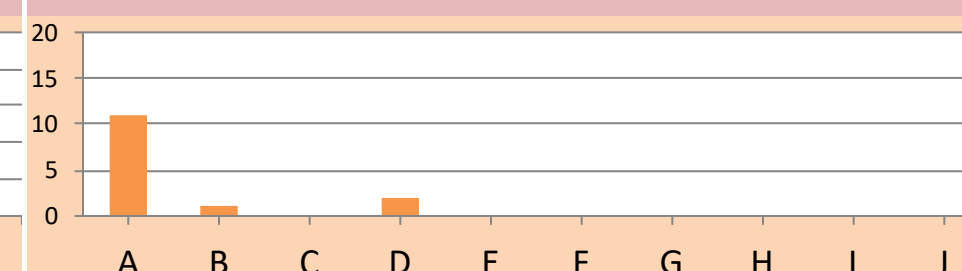
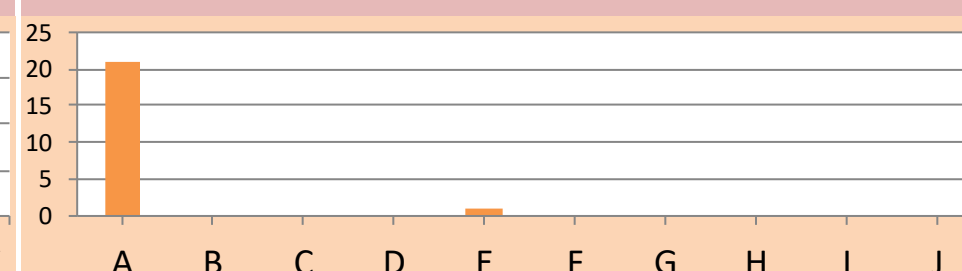
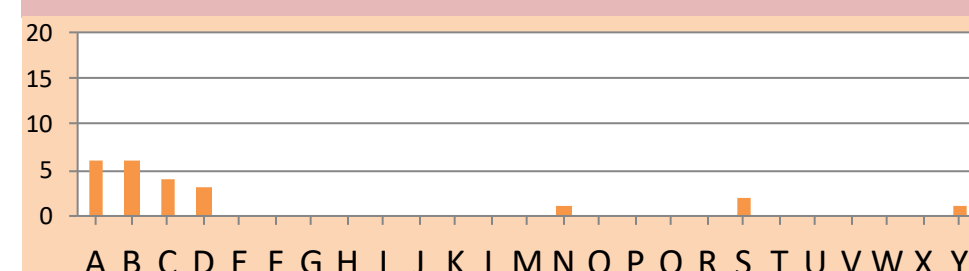
MHco3(ISE)



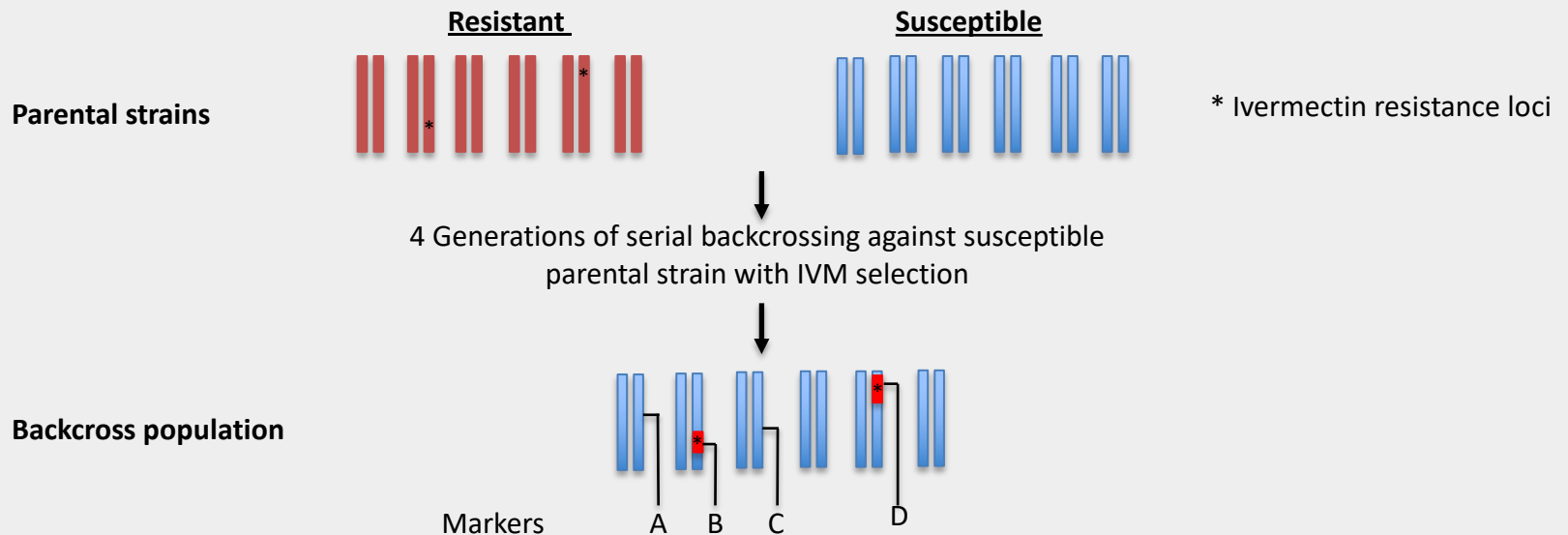
MHco10(CAVR)



MHco3/10.BC



## A Schematic representation of the genomes of parental and backcrossed populations



## B Predictions for haplotype profiles of genetic markers in backcrossed populations

### Hypothetical markers

Markers A and C within “non-introgressed” region

Markers B and D within “introgressed” region

### Overall haplotype frequencies

Not significantly different from susceptible parental strain

Significantly different from susceptible parental strain

### Presence of haplotypes unique to resistant parental strain

Absent (or rare)

One or more present (moderate or high frequency)

**Table 1.** Summary of the results of sequencing data for cloned PCR products for each candidate locus from each of the *Haemonchus contortus* parental and backcross strains.

	Strain	Hcms8a20	<i>Hco-glc-5</i>	<i>Hco-avr-14</i>	<i>Hco-lgc-37</i>	<i>Hco-pgp-9</i>	<i>Hco-pgp-2</i>	<i>Hco-dyf-7</i>	Mean
Number of clones sequenced	MHco3(ISE)	21	23	23	24	24	22	16	22.00
	MHco4(WRS)	22	24	21	24	24	13	13	19.83
	MHco3/4.BC	23	21	22	24	23	18	16	20.67
	MHco10(CAVR)	24	23	21	23	23	17	16	20.50
	MHco3/10.BC	23	23	22	24	23	22	14	21.33
Number of distinct haplotypes observed in each strain	MHco3(ISE)	3	3	5	4	5	3	1	3.50
	MHco4(WRS)	4	9	8	9	13	5	6	8.33
	MHco3/4.BC	3	1	4	4	3	5	2	3.17
	MHco10(CAVR)	5	6	6	6	9	5	3	5.83
	MHco3/10.BC	4	4	3	7	7	2	3	4.33
	Total no. of distinct haplotypes	9	16	17	18	25	10	10	16.00
Shared vs. unique haplotypes for MHco3(ISE) and MHco4(WRS) parental strains	Shared	1	2	1	2	2	2	1	1.67
	Unique to MHco3(ISE)	2	1	4	2	3	1	0	1.83
	Unique to MHco4(WRS)	3	7	7	7	11	3	5	6.67
Shared vs. unique haplotypes for MHco3(ISE) and MHco10(CAVR) parental strains	Shared	0	2	1	1	3	1	1	1.50
	Unique to MHco3(ISE)	3	1	4	3	2	2	0	2.00
	Unique to MHco10(CAVR)	5	4	5	5	6	4	2	4.33

**Table 2.** Pairwise Fst values between the susceptible *Haemonchus contortus* MHco3(ISE) parental strain and MHco4(WRS) and MHco10(CAVR) resistant parental strains. Associated *P* values are shown in parentheses.

Pairwise Comparison	Hcms8a20	<i>Hco-glc-5</i>	<i>Hco-avr-14</i>	<i>Hco-lgc-37</i>	<i>Hco-pgp-9</i>	<i>Hco-pgp-2</i>	<i>Hco-dyf-7</i>
MHco3(ISE)-MHco4(WRS)	0.382 (0.000) <sup>a</sup>	0.340 (0.000) <sup>a</sup>	0.120 (0.000) <sup>a</sup>	0.078 (0.009) <sup>a</sup>	0.163 (0.000) <sup>a</sup>	0.281 (0.000) <sup>a</sup>	0.484 (0.000) <sup>a</sup>
MHco3(ISE)-MHco10(CAVR)	0.358 (0.000) <sup>a</sup>	0.533 (0.000) <sup>a</sup>	0.166 (0.000) <sup>a</sup>	0.108 (0.000) <sup>a</sup>	0.140 (0.000) <sup>a</sup>	0.253 (0.000) <sup>a</sup>	0.367 (0.002) <sup>a</sup>

<sup>a</sup> *P* < 0.05 was considered statistically significant.

**Table 3.** Pairwise  $F_{st}$  values between the susceptible *Haemonchus contortus* MHco3(ISE) parental strain and MHco3/4.BC and MHco3/10.BC backcross strains. Associated  $P$  values are shown in parentheses.

Pairwise Comparison	Hcms8a20	<i>Hco-glc-5</i>	<i>Hco-avr-14</i>	<i>Hco-lgc-37</i>	<i>Hco-pgp-9</i>	<i>Hco-pgp-2</i>	<i>Hco-dyf-7</i>
MHco3(ISE)-MHco3/4.BC	0.383 (0.000) <sup>a</sup>	0.095 (0.063)	0.000 (0.676)	0.115 (0.000) <sup>a</sup>	0.055 (0.135)	0.220 (0.004) <sup>a</sup>	0.000 (0.999)
MHco3(ISE)-MHco3/10.BC	0.512 (0.000) <sup>a</sup>	0.000 (0.514)	0.003 (0.225)	0.000 (0.450)	0.025 (0.153)	0.014 (0.371)	0.117 (0.108)

<sup>a</sup>  $P < 0.05$  was considered statistically significant.

**Supplementary Table S1.** Forward and reverse primers and the PCR product length for each amplicon marker are shown. The length of each genome scaffold on which each amplicon marker is located in the most recent version of the *Haemonchus contortus* MHco3(ISE) genome assembly (as of June 2014; made available by James Cotton and Matt Berriman of the Wellcome Trust Sanger Institute (WTSI), UK) is indicated.

Locus	Amplicon length (bp)	Forward primer (5'-3') - Exon	Reverse primer (5'-3') - Exon	Size of scaffold (kbp)
Hcms8a20	725	GAAGCGGCTCAGATGATAAAGG -not exonic	TTACCGAGGGACTCCGAATG - not exonic	27
<i>Hco-glc-5</i>	420	CCGGCTCGGGTTACGCT - exon 5	CTTGTCGTGAGTCTGGATTC - exon 3	14,479
<i>Hco-avr-14</i>	490	TCGTAGTGTGGCGACCAG - exon 10	CAACGGGTAGAACTCCAATG - exon 8	6,538
<i>Hco-lgc-37</i>	270	GGTGATGTCATGGGTGTC - exon 7	TTGCTGCGAATACGAATC - exon 9	94
<i>Hco-pgp-1</i>	790	AAGTACCATAATCCAGTTGTTAC - exon 11	CAGCAAGAGAATTTTCGGATC - exon 14	6,023
<i>Hco-pgp-2</i>	450	ACCTACGCTGTTGCCGGTGC - exon 7	GTGCCGAGAGCTGCTGAGCC - exon 10	12,643
<i>Hco-dyf-7</i>	690	TCTTCCAGTGGACGAGGTGTCA - exon 8	AGAGGTCGTCCATCAGTGCTTCT - exon 5	11,346

**Supplementary Table S2.** Chromosomal assignment (in bold) of *Caenorhabditis elegans* orthologues of the gene models adjacent to each candidate *Haemonchus contortus* (*Hco*) gene on their respective genome assembly scaffolds.

Chromosome	<i>Hco-glc-5</i>	<i>Hco-avr-14</i>	<i>Hco-lgc-37</i>	<i>Hco-pgp-9</i>	<i>Hco-pgp-2</i>	<i>Hco-dyf-7</i>
I	<b>5</b>	<b>12</b>	0	1	<b>6</b>	0
II	0	0	0	0	0	0
III	0	0	<b>3</b>	3	0	0
IV	0	0	0	<b>4</b>	0	0
V	0	0	0	2	0	0
X	0	0	0	0	0	<b>10</b>
No homology	10	3	3	5	9	5
Total	15	15	6	15	15	15